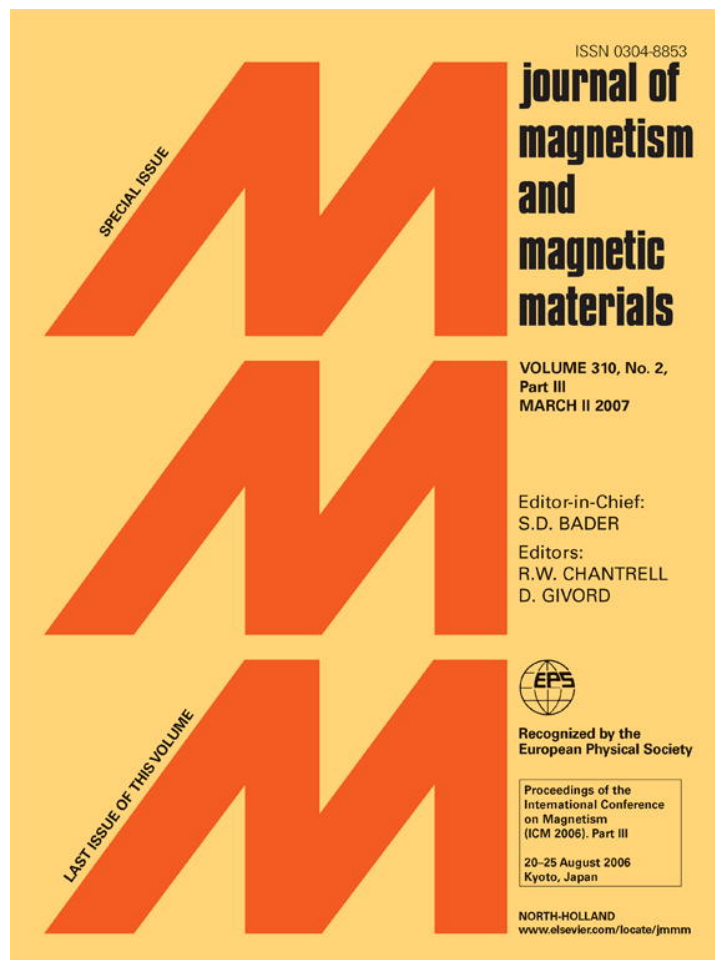


Provided for non-commercial research and educational use only.
Not for reproduction or distribution or commercial use.



This article was originally published in a journal published by Elsevier, and the attached copy is provided by Elsevier for the author's benefit and for the benefit of the author's institution, for non-commercial research and educational use including without limitation use in instruction at your institution, sending it to specific colleagues that you know, and providing a copy to your institution's administrator.

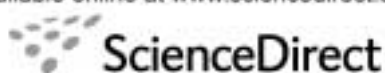
All other uses, reproduction and distribution, including without limitation commercial reprints, selling or licensing copies or access, or posting on open internet sites, your personal or institution's website or repository, are prohibited. For exceptions, permission may be sought for such use through Elsevier's permissions site at:

<http://www.elsevier.com/locate/permissionusematerial>



ELSEVIER

Available online at www.sciencedirect.com



Journal of Magnetism and Magnetic Materials 310 (2007) 2448–2450



www.elsevier.com/locate/jmmm

Effect of anisotropy in magnetic nanotubes

J. Escrig^a, P. Landeros^a, D. Altbir^a, E.E. Vogel^{b,*}

^aDepartamento de Física, Universidad de Santiago de Chile, USACH, Av. Ecuador 3493, Santiago, Chile

^bDepartamento de Ciencias Físicas, Universidad de la Frontera, Casilla 54-D, Temuco, Chile

Available online 17 November 2006

Abstract

Analytical expressions for the total magnetic energy of two characteristic internal configurations of nanometric tubes are calculated. A magnetic phase diagram with respect to the aspect ratio of the tubes is obtained considering anisotropy properties of four materials: iron, cobalt, permalloy and nickel. Conditions for low/high coercive field are discussed.

© 2006 Elsevier B.V. All rights reserved.

PACS: 75.30.Gw; 75.40.Mg; 75.75.+a

Keywords: Nanomagnetism; Nanotubes; Anisotropy

During the last decade, magnetic properties of nanoparticles have been deeply investigated. Different geometries have been considered, including wires, tubes, rings and dots. In particular, magnetic nanotubes may be suitable for applications in biotechnology, where magnetic nanostructures which can float in solutions are very desirable [1]. In order to understand the switching properties of these elements it is of basic importance to establish the role of their geometrical parameters.

Geometrically, magnetic nanotubes are characterized by their external and internal radii, R and a , respectively, and height (or length), H . These particles present two characteristic ideal internal configurations according to their magnetization: parallel to the tube axis F , and concentric to the tube axis V [2–4]. The latter is the vortex state, where magnetic moments lay parallel to the tube basis and circulate around its axis. In this work we consider an isolated magnetic nanotube, which in the case of an array corresponds to sufficiently large separation between the tubes. In this situation, the interaction between them can be ignored. We are interested in determining the range of values for R , a and H where F or V states are favored. Namely, we look for a phase diagram for rather narrow tubes, where there is no core magnetization [4].

We adopt a simplified description of the system, in which the discrete distribution of magnetic moments is replaced by a continuous one characterized by the magnetization $\vec{M}(\mathbf{r})$. The internal magnetic energy, E_{tot} , of a single tube is given by the sum of three terms corresponding to the magnetostatic (E_{dip}), the exchange (E_{ex}) and the anisotropy (E_{k}) contributions. In any case, the dipolar term can be written as

$$E_{\text{dip}} = \frac{\mu_0}{2} \int_V \vec{M}(\mathbf{r}) \cdot \nabla U(\mathbf{r}) \, dv, \quad (1)$$

where $U(\mathbf{r})$ is the magnetostatic potential.

The magnetization is regarded as varying slowly on the scale of the lattice parameter. Therefore, the exchange term takes the form [5]:

$$E_{\text{ex}} = A \int_V ((\nabla m_x)^2 + (\nabla m_y)^2 + (\nabla m_z)^2) \, dv, \quad (2)$$

where $m_i = M_i/M_0$ is the normalized component of the magnetization with respect to the saturation magnetization M_0 and A is the stiffness constant of the material. In Eq. (2) a constant term, independent of the configuration, has been left out [5].

The cubic anisotropy energy of the particle can be added by means of the following expression:

$$E_c = K_c \int_V (m_x^2 m_y^2 + m_y^2 m_z^2 + m_z^2 m_x^2) \, dv, \quad (3)$$

*Corresponding author. Tel.: +56 45 325316.
E-mail address: ee_vogel@ufro.cl (E.E. Vogel).

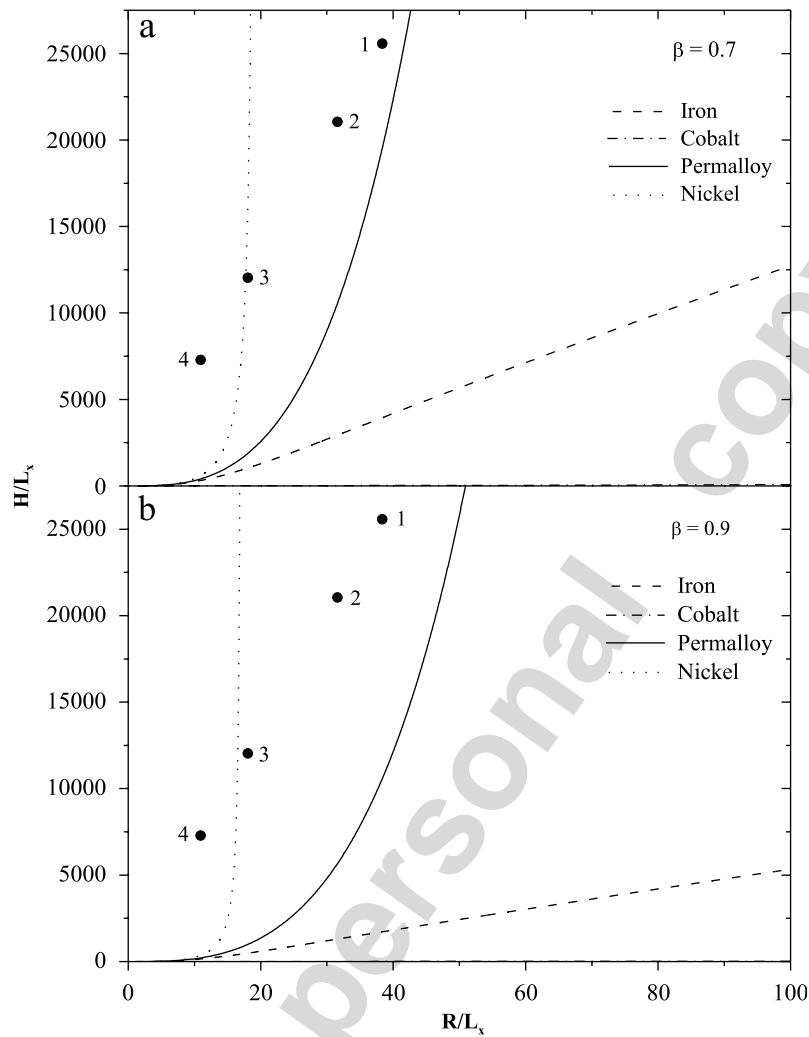


Fig. 1. Phase diagrams for magnetic nanotubes giving the regions in the RH plane where one of the configurations has lower energy: F phase to the upper left, V phase to the lower right. Points 1, 2, 3 and 4 are discussed in the text.

and the uniaxial anisotropy energy is given by

$$E_u = -K_u \int_V m_z^2 dv. \quad (4)$$

We now proceed to the calculation of the various energy terms. Results are given in units of $\mu_0 M_0^2 L_x^3$, that is to say $\tilde{E} = E/\mu_0 M_0^2 L_x^3$. In this case we have used the exchange length given by $L_x = \sqrt{2A/\mu_0 M_0^2}$.

For the F parallel configuration, $\vec{M}(\mathbf{r})$ can be approximated by $M_0 \hat{z}$, where \hat{z} is the unit vector parallel to the axis of the nanotube, and the reduced energy reads

$$\begin{aligned} \tilde{E}^F = & \frac{\pi R^3}{L_x^3} \int_0^\infty \frac{dq}{q^2} (1 - e^{-qV}) [J_1(q) - \beta J_1(q\beta)]^2 \\ & - \frac{\kappa_u}{2} \frac{\pi H R^2}{L_x^3} (1 - \beta^2). \end{aligned} \quad (5)$$

Here, $\beta = a/R$, $\gamma = H/R$ and $\kappa_u = 2K_u/\mu_0 M_0^2$. In this expression $J_1(z)$ are Bessel functions.

For the V configuration the magnetization can be approximated by $M_0 \hat{\phi}$. In such case the contribution from the dipolar energy equals zero, and

$$\tilde{E}^V = -\frac{\pi H}{L_x} \ln \beta + \frac{\kappa_c}{16} \frac{H R^2}{L_x^3} \pi (1 - \beta^2). \quad (6)$$

Here, $\kappa_c = 2K_c/\mu_0 M_0^2$. Eqs. (5) and (6) were previously obtained [4] for $K_c = K_u = 0$.

We proceed to investigate the relative stability of the configurations. Phase diagrams are shown in Fig. 1 for two values of β that are appropriate for narrow tubes, namely, 0.7 and 0.9. Anisotropy for four different materials are considered according to values presented in Table 1. Each line separates the F configuration (upper left) from the V configuration (lower right). Notice that for the case of Co the transition line is very close to the abscissa axis and then the F phase is present in almost all the range studied here. Because of its very low anisotropy, results for permalloy describe reasonably well a material with no anisotropy, as it was considered in Ref. [4].

Table 1
Parameters for different materials taken from Ref. [6]

Material	M_0 (A/m)	L_x (nm)	K (J/m ³)	κ
Iron	1.7×10^6	2.346	4.8×10^4	0.0264
Cobalt*	1.4×10^6	2.849	4.1×10^5	0.3329
Permalloy	8.0×10^5	4.986	-3.0×10^2	-0.0007
Nickel	4.85×10^5	8.225	-4.5×10^3	-0.0304

For all these materials, $A \sim 10^{-11}$ J/m. Uniaxial (K_u) cobalt is denoted with a superscript *. Iron, permalloy and nickel have cubic (K_c) anisotropy.

As a specific illustration we did calculations for magnetic nanotubes with $R = 90$ nm and $H = 60 \mu\text{m}$ [1] made of the materials characterized in Table 1. Results are presented in Fig. 1 as dots: Fe: 1, Co: 2, permalloy: 3 and Ni: 4. The Ni dot is closer to the transition line than the other cases. This is an indication for a lower coercive field. On the contrary, the other cases are well inside the F phase and should have a large coercive field.

In conclusion, we have investigated the role of anisotropy energy in the phase diagram obtained for different geometries. We have shown that anisotropy plays a fundamental role in the ground state of magnetic tubes. The magnetic state of nanotubes depends strongly on the material used as well as on each of the geometrical features

defining the tube. Thus, if one looks for low-coercive devices the best bet seems to be Ni, with R/L_x about 10 and almost any H/L_x ; this condition is favored for thinner tubes (β close to 1.0). On the contrary, cobalt will always present high coercivity, almost independently of the aspect ratio of the particle.

This work has been partially supported by Fondo Nacional de Investigaciones Científicas y Tecnológicas (FONDECYT, Chile) under Grants nos. 1050013 and 1060317, and Millennium Science Nucleus “Condensed Matter Physics” P02-054F of Chile. CONICYT Ph.D. Program Fellowships is gratefully acknowledged.

References

- [1] K. Nielsch, F.J. Castaño, S. Matthias, W. Lee, C.A. Ross, *Adv. Eng. Mater.* 7 (2005) 217.
- [2] P. Landeros, J. Escrig, D. Altbir, J. d’Albuquerque e Castro, P. Vargas, *Phys. Rev. B* 71 (2005) 94435.
- [3] Y.C. Sui, R. Skomski, K.D. Sorge, D.J. Sellmyer, *Appl. Phys. Lett.* 84 (2004) 1525.
- [4] J. Escrig, P. Landeros, D. Altbir, E. E. Vogel, P. Vargas, *J. Magn. Magn. Mater.* 308 (2007) 233.
- [5] A. Aharoni, *Introduction to the Theory of Ferromagnetism*, Clarendon Press, Oxford, 1996.
- [6] R.C. O’Handley, *Modern Magnetic Materials*, Wiley, New York, USA, 2000.